Available online at www.sciencedirect.com
ScienceDirect
Biomaterials 29 (2008) 1912–1919
Biomaterials
www.elsevier.com/locate/biomaterials

Particle size-dependent organ distribution of gold nanoparticles after intravenous administration

Wim H. De Jong [a,*], Werner I. Hagens [b], Petra Krystek [c,1], Marina C. Burger [a], Adriënne J.A.M. Sips [b], Robert E. Geertsma [d]

[a] *Laboratory for Health Protection Research, National Institute for Public Health and the Environment (RIVM), Antonie van Leeuwenhoeklaan 9, PO Box 1, 3720 BA Bilthoven, The Netherlands*
[b] *Centre for Substances and Integrated Risk Assessment, RIVM, The Netherlands*
[c] *DSM Resolve, PO Box 18, 6160 MD Geleen, The Netherlands*
[d] *Centre for Biological Medicines and Medical Technology, RIVM, The Netherlands*

Received 6 September 2007; accepted 11 December 2007
Available online 1 February 2008

Abstract

A kinetic study was performed to determine the influence of particle size on the in vivo tissue distribution of spherical-shaped gold nanoparticles in the rat. Gold nanoparticles were chosen as model substances as they are used in several medical applications. In addition, the detection of the presence of gold is feasible with no background levels in the body in the normal situation. Rats were intravenously injected in the tail vein with gold nanoparticles with a diameter of 10, 50, 100 and 250 nm, respectively. After 24 h, the rats were sacrificed and blood and various organs were collected for gold determination. The presence of gold was measured quantitatively with inductively coupled plasma mass spectrometry (ICP-MS).

For all gold nanoparticle sizes the majority of the gold was demonstrated to be present in liver and spleen. A clear difference was observed between the distribution of the 10 nm particles and the larger particles. The 10 nm particles were present in various organ systems including blood, liver, spleen, kidney, testis, thymus, heart, lung and brain, whereas the larger particles were only detected in blood, liver and spleen. The results demonstrate that tissue distribution of gold nanoparticles is size-dependent with the smallest 10 nm nanoparticles showing the most widespread organ distribution.

Keywords: Nanoparticles; Biodistribution; Biocompatibility; Toxicokinetics

1. Introduction

Nanoscience can be defined as the study of phenomena and manipulation of materials at atomic, molecular and macromolecular scales where physico-chemical properties may differ significantly from those at a larger particulate scale. Nanotechnology is then the design, characterization, production and application of structures, devices and systems by controlling the shape and size at the nanometer scale [1]. The fast growing number of applications of engineered nanoparticles in drug delivery systems, medical devices, food products, consumer products and the subsequent disposal of engineered nanoparticles in the environment imply that human exposure to engineered nanoparticles is expected to increase greatly. Engineered nanoparticles show remarkable structural diversity, each structure exhibiting their own individual characteristics, such as tubes, dots, wires, fibres and capsules [2–4]. The size at which the different structures change their properties is not a generally applicable limit value, but it probably differs from compound to compound. Although no scientifically accepted definition exists, in general the nanoscale applies to

* Corresponding author. Tel.: +31 30 2742311; fax: +31 30 2744446.
E-mail address: wim.de.jong@rivm.nl (W.H. De Jong).
[1] Current address: MiPlaza Materials Analysis, Philips Research, High Tech Campus 12, 5656 AE Eindhoven, The Netherlands.

0142-9612/$ - see front matter © 2008 Elsevier Ltd. All rights reserved.
doi:10.1016/j.biomaterials.2007.12.037

the structures having at least one dimension at a size in the order of 100 nm or less. However, for regulatory purposes the 100 nm threshold is of limited value, as there is no reason to assume that 100 nm would be an absolute threshold for changes in the physico-chemical properties of nanoparticles.

The specific physico-chemical properties at the nanoscale are expected to result in increased reactivity with biological systems. So, in addition to their beneficial effects, engineered nanoparticles of different types may also represent a potential hazard to human health. Several studies indeed suggest that these nanoparticles have a different toxicity profile compared with larger particles [5,6].

Kinetic properties are considered to be an important descriptor for potential human toxicity and thus for human health risk. It is important to know the amount of the total external exposure that will be absorbed by the body and result in an internal exposure. In addition, the distribution of absorbed nanoparticles inside the body over the various organ systems and within the organs needs to be determined. After the initial absorption of nanoparticles the systemic circulation can distribute the particles towards all organs and tissues in the body. Several studies have shown distribution of particles to multiple organs including liver, spleen, heart and brain [7–10].

As a model particle for nanotechnology research, metallic colloidal gold nanoparticles are widely used. They can be synthesized in different forms (rods, dots), are commercially available in various size ranges and can be detected at low concentrations. It has been reported that human cells can take up gold nanoparticles without cytotoxic effects [11]. In particular for biomedical applications, they can be considered relevant models, since they are used as potential carriers for drug delivery, imaging molecules and even genes [12], and for the development of novel cancer therapy products [13–17]. In addition, they have a history as label for tracking protein distribution in vivo in which proteins are coupled to small colloidal gold beads at nanoscale dimensions [18].

Hillyer and Albrecht [7] showed that after oral administration of metallic colloidal gold nanoparticles of decreasing size (58, 28, 10 and 4 nm) to mice an increased distribution to other organs was observed. The smallest particle (4 nm) administered orally resulted in an increased presence of gold particles in kidney, liver, spleen, lungs and even the brain. The biggest particle (58 nm) tested was detected almost solely inside the gastrointestinal tract. For 13 nm sized colloidal gold beads the highest amount of gold was observed in liver and spleen after intraperitoneal administration [18]. In another study, intravenously injected gold nanorods (length 65 ± 5 nm; width 11 ± 1 nm) revealed that within 30 min these particles accumulated predominantly in the liver. The PEGylation (coating with polyethylene glycol) of these gold nanorods resulted in a prolonged circulation [19].

The aim of our study was to determine the influence of particle size on the in vivo tissue distribution of gold nanoparticles in the rat. To circumvent the absorption process, rats were intravenously injected with solutions containing various sized metallic colloidal gold nanoparticles (10, 50, 100 and 250 nm).

2. Animals, materials and methods

2.1. Animals

Male WU Wistar-derived rats, 6–8 weeks of age were obtained from the animal facility of the Institute (RIVM, Bilthoven, The Netherlands). Animals were bred under SPF conditions and barrier maintained during the experiment. Drinking water and conventional feed were provided *ad libitum*. Husbandry conditions were maintained according to all applicable provisions of the national laws, Experiments on Animals Decree and Experiments on Animals Act. The experiment was approved by an independent ethical committee prior to the study.

2.2. Experimental design

Gold nanoparticles of 10, 50, 100 and 250 nm in aqueous suspension were obtained from SPI supplies, West Chester, PA, USA. The characteristics of the gold nanoparticles are presented in Table 1. The gold suspensions were 10% diluted by adding one part of 10 times concentrated phosphate buffered saline ($10 \times$ PBS) to nine parts of the gold suspension, in order to obtain a physiological solution for intravenous injection. Directly after PBS addition the nanoparticle solutions of 10, 50 and 100 nm showed a change in colour from red to blue indicating the formation of nanoparticles agglomerates/aggregates, whereas the 250 nm particles did not. The solutions remained clear and no sediments or agglomerates/aggregates were visually noted. A PBS control solution was prepared by adding one part of $10 \times$ PBS to nine parts of distilled water (1:10). Three experiments were performed. In experiment 1 ($N = 4$) 10 and 100 nm particles, in experiment 2 ($N = 4$) 10 and 250 nm particles,

Table 1
Characteristics of gold nanoparticles

Characteristics of gold nanoparticles per particle solution				
	10 nm	50 nm	100 nm	250 nm
Gold particle size (nm)	9.5	48.2	99.9	247.8
Size distribution (%)	<10	<8	<8	<8
Number of particles in injection solution (/ml)	5.1E + 12	4.0E + 10	5.0E + 09	3.2E + 08
Surface area particle (nm^2)	284	7299	31,353	192,909
Surface area injection solution (nm^2/ml)	1.45E + 15	2.96E + 14	1.58E + 14	6.25E + 13
Gold concentration injection solution (μg/ml)	77	96	89	108
Gold concentration as measured by ICP-MS (μg/g sample)	80	107	106	120

and in experiment 3 ($N = 15$) 10, 50, 100, 250 nm particles and PBS were used, respectively. One ml of each freshly prepared solution was injected in the tail vein. The injections were well tolerated and no adverse effects were observed during the 24 h observation period.

At 24 h after injection blood and the following organs were collected: adrenals, aorta, brain, heart, kidney, liver, lung, lymph nodes (mesenteric and popliteal), spleen, testis, thymus, and vena cava. Organs were weighed, and tissue samples were homogenized and frozen for determination of gold content by inductively coupled plasma mass spectrometry (ICP-MS). EDTA blood was collected and stored in the refrigerator (4–7 °C).

2.3. Reagents, standards, and reference materials

All chemicals used were of analytical grade or of high purity. Nitric acid (HNO_3) and hydrochloric acid (HCl) were purchased from Merck, Darmstadt, Germany. Calibration standard solutions of gold (Au), copper (Cu) and zinc (Zn) as well as solutions of the element used as internal standard, rhodium (Rh), were made of single element stock solutions with a concentration of 1000 μg/mL from Merck, Darmstadt, Germany. Deionised water (H_2O) was purified by a Millipore system (Milli-Q, 18.2 MΩcm). The certified reference material "BCR 186 Pig Kidney" was supplied by C.N. Schmidt, Amsterdam, The Netherlands.

2.4. Instrumentation

The sample material of organs, blood and original solutions of gold nanoparticles was digested by using a microwave system CEM Mars 5 (CEM, Kamp Lintfort, Germany). The presence of elemental gold was measured with an inductively coupled plasma mass spectrometer (ICP-MS, type Agilent 7500 CE, Agilent Technologies, Waldbronn, Germany). Transmission electron microscopy (TEM) was performed using a FEI Company Tecnai 12 (FEI Company, Eindhoven, The Netherlands) transmission electron microscope.

2.5. Accuracy and quality control aspects of ICP-MS

Four types of experiments were included to cover different performance characteristics and quality control aspects. For gathering details about inhomogeneity in the sample material, several liver tissue samples were analysed as independent duplicates. For control on the digestion procedures, chemical blanks and a certified reference material were analysed. However, for gold in biological materials there is no suitable reference material commercially available. Therefore "BCR 186 Pig Kidney" was chosen to represent a comparable matrix (kidney) and the two certified elements (Cu and Zn) were analysed. The matrix effects were also studied by the standard addition experiments and the calculation of the recovery. The digested solution of BCR 186 was spiked prior to the measurement with known concentrations (0.2–0.5 μg/L) of the gold standard solution which was also used for the external calibration. Finally, standard addition experiments were carried out by spiking blood samples of non-treated control rats with the nanoparticles (10, 50, 100, 250 nm) prior to sample pretreatment and analysis.

2.6. Sample preparation prior to measurement with ICP-MS

Homogenized organ samples (0.5 g) were weighed into a digestion vial of the microwave system. For other matrices the sample amount was as follows: 0.2 g blood 24 h; 0.1 g blood 5 min; and 0.1 g original nanoparticles (10, 50, 100, 250 nm). Into the digestion vial 9 mL of aqua regia (6 mL HCl conc. and 2 mL HNO_3 conc.) was added. The mixture was treated under microwave conditions, which are presented in Table 2. Afterwards the mixture was transferred to another vial, and H_2O was added to a total volume of 25 mL. The total solution was shortly shaken by hand.

For tissue samples of the adrenal glands, lymph nodes and blood vessels (aorta and vena cava) with a weight below 0.3 g, this method of sample preparation could not be used. Cold dissolution of these samples with aqua regia led to insufficient results.

Table 2
Program for tissue digestion with microwave system

Stage	Ramp to T (W (100%))	Ramp (min)	°C	Hold (min)
1	1200	15	140	0
2	1200	15	190	30

2.7. Measurement with ICP-MS

Prior to the measurement aliquots were spiked with the internal standard Rh (final concentration: 10 μg/L) and diluted to approximately 0.5% HCl in solution.

The quantification was carried out by external five-point-calibration with internal standard correction. Stock solutions were diluted with approximately 0.5% HCl to relevant concentration levels. All measurements of standards and samples were carried out with the ICP-MS system. The main instrumental operating conditions are as follows: RF power 1500 W, carrier gas flow 0.85 L/min Ar and makeup gas flow 0.19 L/min Ar. The following isotopes were measured: ^{197}Au and ^{103}Rh as internal standard, and ^{63}Cu and ^{66}Zn were measured for the quality control aspects of BCR 186.

2.8. TEM

Samples of nanoparticle suspensions used for intravenous administration were prepared for evaluation by transmission electron microscopy. Samples were added to a carbon-coated formvar film, contrasted with 2% phosphotungsten acid (pH = 5), and allowed to dry. Without further preparation the samples were evaluated in a transmission electron microscope.

3. Results

3.1. Gold nanoparticles characteristics and general quality control aspects

The total amount of elemental gold injected was determined with ICP-MS. The gold concentration as determined by calculation using the information of the manufacturer and the dilution factor was compared with the gold concentration measured by ICP-MS. There was a maximum of 20% deviation of the claimed concentration. Table 1 shows the characteristics of the different sized nanoparticles in the injection solution per volume. The results of the quality control aspects of ICP-MS are given in Table 3. These results are sufficient for covering aspects related to reliable measurements of gold in the selected biological matrices.

3.2. Blood and organ distribution

In most animals elemental gold could be detected at 24 h after intravenous injection, the amount ranging from 588 to 2656 ng/g blood. Animals, in which for the liver as determined by ICP-MS at 24 h a minimal (<2% of the injected dose) or no detectable level of gold was observed, clearly identifying them as outliers, were not included in the evaluation ($N = 1$ in the 50 nm group, and $N = 1$ in the 100 nm group). The results of the gold measurements in the various organs are presented in Table 4. In the blood, liver and spleen the absolute amount of gold detected as expressed as ng/g organ is highest, while the amount measured in other organs is much lower. An

Table 3
Results of quality control aspects of ICP-MS

Experiment	Result
Independent duplicates ($N = 2$) of liver tissue samples: particles sized	
10 nm:	2202 ng/g liver (±18%)
	1572 ng/g liver (±22%)
100 nm:	3473 ng/g liver (±1.0%)
	2472 ng/g liver (±1.2%)
BCR 186 Pig Kidney ($N = 2$): recovery of the certified concentration of	
Cu:	80 ± 2%
Zn:	99 ± 2%
Standard addition of gold standard solution to BCR 186 ($N = 1$): recovery of	
0.2 μg/L Au:	96%
0.5 μg/L Au:	107%
Standard addition of gold nanoparticles to blood ($N = 1$): recovery of particles sized	
10 nm:	95%
50 nm:	89%
100 nm:	111%
250 nm:	134%

exception is the amount of gold in the lungs of animals treated with 50 nm gold nanoparticles. The 10 nm gold nanoparticles show the most widespread presence in the various organ systems including brain, heart, kidneys, lungs, testis, and thymus (Table 4). The concentration in the liver was found to be the highest, followed by the spleen. In the brain of one of the control rats (no gold injected), a low but detectable concentration of gold was measured.

If we calculate the amount of gold detected as a percentage of the injected dose, the highest percentages recovered are present in blood and liver adding up to approximately 70–80% of the injected dose, at 24 h after injection (Table 5). The majority of the nanoparticles accumulate in the liver after intravenous injection irrespective of the size of the nanoparticles. Twenty-four hours after injection, 46 ± 7% of the total injected 10 nm, 21 ± 5% of the 50 nm, 44 ± 1% of the 100 nm and 31 ± 5% of the 250 nm gold particles were located in the liver. The percentage recovery of the injected gold particles in the spleen was 2.2 ± 0.2% for 10 nm, 1.3 ± 0.3% for the 50 nm, 1.4 ± 0.3% for 100 nm and 1.2 ± 0.3% for the 250 nm gold particles (Table 5).

For the injected 10 nm particles, the percentage of the dose, located in the kidneys (1.0%), brain (0.3%), reproductive organs, thymus and heart (all 0.2%) was much higher than for the 50, 100 and 250 nm gold particles (if detected at all for these particles). For the lungs, the amount of gold measured after injection of the 50 nm gold particles is relatively high, whereas 100 and 250 nm particles hardly were detected in this organ. The high amount in the lung was due to a high content in one out of the two animals which were evaluated for the 50 nm gold particles, which also resulted in a high standard deviation. Interestingly there were hardly any differences in distribution between the 100 and 250 nm particles seen in this experiment. As a negative control, three rats were injected with PBS alone. No gold was detected in the organs of these animals with an exception of the brain, where a low but detectable amount of gold was measured in one animal.

With the exception of blood and liver, the percentage of the dose distributed to the various organs seems low. However, this small percentage represents a very large number of particles. In Table 6, the average number of particles is presented as they are distributed in the rats.

3.3. TEM evaluation

Samples of nanoparticle suspensions of 10, 50, 100 and 250 nm were evaluated by TEM. The 10 nm sample showed mainly individual nanoparticles and some clusters in which up to 60 nanoparticles could be counted (Fig. 1). The nanoparticles in the cluster were loosely arranged and individual nanoparticles could be easily recognised, indicating that the clusters consisted of agglomerates with weakly binding forces. In samples of nanoparticles of 50, 100 and 250 nm individual nanoparticles and some clusters of 2–8 nanoparticles were observed (Fig. 1).

4. Discussion

In this study, we compared the tissue distribution of various sized gold nanoparticles in the rat. Although the study was

Table 4
The concentration of gold measured in the organs (expressed as ng/g organ)

Tissue	10 nm, Concentration gold (ng/g organ)		50 nm, Concentration gold (ng/g organ)		100 nm, Concentration gold (ng/g organ)		250 nm, Concentration gold (ng/g organ)		Blank, concentration gold (ng/g organ)
	Mean	SEM	Mean	SEM	Mean	SEM	Mean	SEM	Mean
Blood	1486	340	1352	308	2161	385	969	22	Nd
Liver	2700	400	1211	236	3268	266	3008	451	Nd
Spleen	2225	205	1358	458	1793	398	1991	462	Nd
Lungs	188	62	1740	1184	44	44	35	39	Nd
Kidneys	343	158	58	22	30	19	26	19	Nd
Testis	55	21	Nd	Nd	Nd	Nd	6	7	Nd
Thymus	205	95	Nd	Nd	6	6	35	39	Nd
Heart	164	82	49	17	9	9	Nd	Nd	Nd
Brain	128	61	Nd	Nd	Nd	Nd	Nd	Nd	18
	$N = 7$		$N = 2$		$N = 4$		$N = 5$		$N = 3$

Nd: not detectable, and SEM: standard error of the mean.

Table 5
The concentration of gold measured in the organs (expressed as % of the given dose)

Tissue	10 nm, Concentration gold % injected dose		50 nm, Concentration gold % injected dose		100 nm, Concentration gold % injected dose		250 nm, Concentration gold % injected dose		Blank, concentration gold
	Mean	SEM	Mean	SEM	Mean	SEM	Mean	SEM	Mean
Blood	36.3	10.4	30.9	7.8	44.5	13.5	16.4	2.9	–
Liver	46.3	6.9	20.8	5.2	44.2	0.9	31.0	5.0	–
Spleen	2.2	0.2	1.3	0.3	1.4	0.3	1.2	0.3	–
Lungs	0.3	0.1	2.3	1.6	–	–	–	–	–
Kidneys	1.0	0.4	0.2	0.1	0.1	–	0.1	–	–
Testis	0.2	0.1	–	–	–	–	–	–	–
Thymus	0.2	0.1	–	–	–	–	–	–	–
Heart	0.2	0.1	0.1	–	–	–	–	–	–
Brain	0.3	0.1	–	–	–	–	–	–	–
	$N=7$		$N=2$		$N=4$		$N=5$		$N=3$

SEM: standard error of the mean.

designed with specific relevance for intravenously administered nanoparticles in medical applications, the results can also be considered useful for other routes of exposure. After absorption of nanoparticles following, e.g. inhalation, oral or dermal exposure, further distribution in the body then occurs via the blood circulation. The distribution of gold nanoparticles proved to depend on the size of the injected particles. The smallest particle studied, 10 nm, revealed the most widespread tissue distribution at 24 h after injection. In contrast to the larger particles, the 10 nm particles were detected in all of the evaluated organs with the ICP-MS measurements. The number of particles found in the liver was the highest, followed by blood, spleen, kidney, lungs, brain, reproductive organs, thymus and heart, whereas the 50, 100 and 250 nm particles revealed almost solely distribution to liver, spleen and blood. Our results are in agreement with results reported previously by Hillyer and Albrecht [18] who found the highest levels of gold in liver and spleen and lower levels in brain, lung, heart, kidney, small intestine and stomach. They used repeated intraperitoneal administration for 4 days with a concentrated gold suspension resulting in a relatively high dose compared to our studies as they observed gold levels in the order of microgram per gram organ whereas we found nanogram per gram organ. Also for gold nanorods the highest level of gold was observed in the liver after intravenous administration [19].

The quantitative ICP-MS results indicated that 0.3% of the injected dose of 10 nm gold particles was distributed to the brain after 24 h. No gold was detected in the brain for the 50, 100 and 250 nm particles by ICP-MS. Our results do not show where the gold was located in the brain. So, we do not know whether the nanoparticles were present in neural tissue and passage of the blood brain barrier did occur. Our ICP-MS results neither confirm nor deny the possibility of blood brain barrier passage.

The ICP-MS measurements indicated in one of the three control rats a very low but detectable concentration of gold in the brain. The other two control rats were negative in all measurements. It is unknown whether this is an incidental artefact or whether the measurement of a very low concentrations of gold with our method is incorrect. In one animal of the 50 nm group, no gold could be detected in the organs, while in one rat of the 100 nm group no gold could be detected in the blood and less that 2% of the injected dose in the liver as determined by ICP-MS after 24 h. These findings are not in line with all other rats ($N=18$) in the experimental groups and these rats were therefore excluded from the evaluation as an unexplained erroneous result.

Table 6
The average number of gold particles distributed to the various organs (estimated)

Tissue	10 nm, Number of particles (number/g organ)	50 nm, Number of particles (number/g organ)	100 nm, Number of particles (number/g organ)	250 nm, Number of particles (number/g organ)
Blood	1.9E + 12	1.2E + 10	2.2E + 09	4.6E + 07
Liver	2.4E + 12	8.2E + 09	2.3E + 09	9.5E + 07
Spleen	1.1E + 11	5.2E + 08	7.3E + 07	3.8E + 06
Lungs	1.4E + 10	9.0E + 08	2.2E + 06	1.2E + 05
Kidneys	4.9E + 10	6.5E + 07	3.8E + 06	1.6E + 05
Testis	1.1E + 10	–	–	4.2E + 04
Thymus	9.1E + 09	–	–	6.4E + 04
Heart	9.9E + 09	2.2E + 07	4.3E + 05	–
Brain	1.6E + 10	–	–	–
	$N=7$	$N=2$	$N=4$	$N=5$

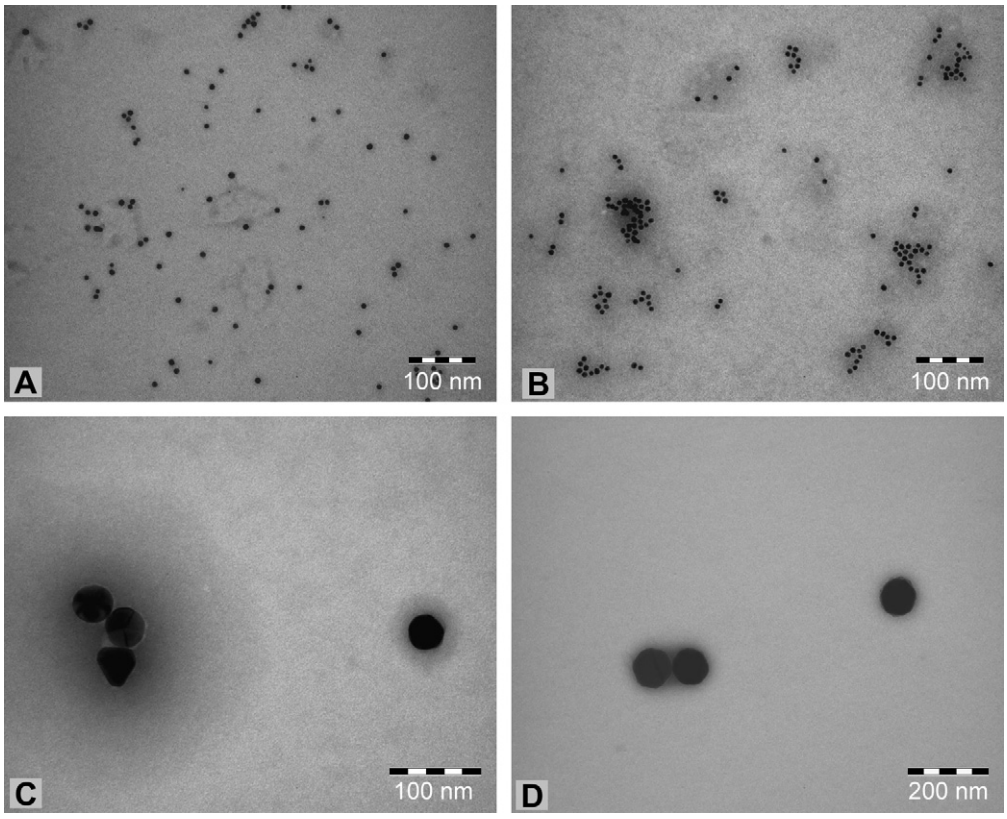

Fig. 1. TEM evaluation of nanoparticle suspensions used for intravenous administration. Fig. 1A and B shows 10 nm particles, (C) 50 nm particles and (D) 100 nm particles. Note for A and B the presence of nanoparticles both as individual particles and groups of particles. (A and B) Magnification ×110,000; (C) magnification ×150,000; and (D) magnification ×67,000.

After 24 h, as much blood as possible was collected from the rats to maximize removal of residual blood from the organs as much as possible. The residual amount of blood present in the organs is not known. Hence, the amount of gold found in organs with a high-blood content (kidneys, heart, liver) could have been overestimated. However, the concentration found in kidney, heart and other blood containing organs is very low, even compared to the concentration found in blood. Moreover, if the amount of residual blood would have been responsible for the detection of the 10 nm gold in the various organs for the other particle sizes similar amounts of gold should have been measured as well. The amount of gold in the blood does not differ greatly between the four sizes of nanoparticles investigated with the exception of the 250 nm particles (Table 4). Therefore, it is assumed that the residual blood in the organs had only a minor effect on the amount of gold measured and is not responsible for the presence of the widespread organ distribution of the 10 nm gold nanoparticles.

We used the ICP-MS method for evaluation of the gold content of the various organs. For some organs (e.g. lymph nodes, vena cava and aorta) the amount of tissue sample was not sufficient for the tissue dissolution method used. ICP-MS has the advantage that you can measure the metal content within an organ, in our assays gold. Our spiking control experiments for the ICP-MS measurements showed a very good recovery for the gold samples. This suggests that the loss of gold content during sample (organ) processing was limited. Previously, it was reported that especially in the very low detection levels ICP-MS may not be the most sensitive method for detection of gold [18]. Instrumental neutron activation analysis (INAA) was reported to be more sensitive [18]. A limitation of this technique may be that it requires a neutron source, is more costly, and has a low sample throughput. In this comparison of ICP-MS and INAA the samples for ICP-MS were not pretreated as we did in our study which may have had an effect on the detection limits. In our study sample pretreatment by acid digestion was found to be essential for optimal detection results. Our results clearly show a difference in tissue distribution between the smallest (10 nm) and largest (250 nm) gold particles investigated. Although only a low percentage (1.0% or less) of the administered dose was observed in organs other than liver and spleen, a low percentage may still be a relatively high number of particles (see Table 6). In addition, a considerable amount was present in the blood at 24 h after injection which may result in further accumulation.

Another method for detecting tissue distribution of injected materials is the use of a radioactive label, which, depending on the label, can be used with a more limited processing method which may limit loss of test sample. Radioactive labeling was used for studying the translocation of ultrafine (nano)particles from the lung into the circulation and organs [9,20–23]. For more complex composed nanoparticles there is, however, the

possibility for losing the label, as was previously discussed for technetium labeled carbon particles used for studying lung passage of inhaled ultrafine particles [9,21,22]. Kreyling et al. [20] and Wiebert et al. [23] found rather low levels of translocation from the lung into the circulation for iridium, while in contrast Oberdörster et al. [10] observed considerable radioactive carbon in the liver indicating a high translocation from the lung. It cannot be excluded that such translocation to blood and extrapulmonary organs may well be dependent on the chemical composition of the ultrafine particles and thus be different for different types of particles. However, one has to realize that even low levels of translocation expressed as percentage of the administered dose still may result in a considerable number of particles in the circulation and thus have the potential for accumulation in organs.

The TEM evaluation of the samples administered revealed the presence of clusters of nanoparticles mainly in the 10 nm sample. The arrangement of the nanoparticles in the sample indicated that the clusters were most likely agglomerates with weak binding forces. After intravenous administration the gold nanoparticles may be covered with various proteins as present in blood such as serum albumin and apolipoproteins as demonstrated for polymeric nanoparticles [24]. These proteins on the nanoparticles may facilitate cellular uptake. Particles are mainly taken up into cells by phagocytic pathways. Previously Geiser et al. [25] and Rothen-Rutishauser et al. [26] demonstrated the presence of different types of nanoparticles (gold and titanium oxide of 25 and 22 nm, respectively) inside red blood cells. They concluded that nanoparticles are able to cross the cell membrane by processes other than phagocytosis and endocytosis since erythrocytes do not have phagocytotic receptors. Diffusion, transmembrane channels, adhesive interactions or other, undefined, transmembrane processes might play a role in this cellular uptake. Moreover, the uptake of ultrafine and 200 nm sized particles in macrophages was not blocked by the phagocytosis inhibitor cytochalasin D, whereas the uptake of 1000 nm (1 μm) particles was inhibited [25], indicating the non-phagocytic nature of the uptake of the smaller nanoparticles.

It is unclear to what extent the various nanoparticle characteristics contribute to their kinetics. Since common kinetic properties cannot be extracted from the available data, more different particle types should be examined carefully. Quantified nanokinetic data are essential to model possible effects. In order to obtain these data, the development of validated detection methods for nanoparticles in biological samples is urgently needed. For translocation from the lung into the vasculature after inhalation different results were obtained for iridium and titaniumdioxide nanoparticles, which also indicates that the chemical composition has an effect on nanoparticle behavior [20,27,28].

This kinetic study was intended to elucidate the effect of size of nanoparticles on the distribution pattern in rats and revealed a size-dependent distribution. However, this study did not include all relevant kinetic processes since the excretion route has not been measured. A time-dependent study design could elucidate the kinetic half-life of the various sized nanoparticles. It would also be interesting to investigate the particle distribution with nanoparticles of the same size tested (10, 50, 100 and 250 nm) but consisting of other core material (e.g. silver, carbon, silica, TiO_2, ZnO) or of other shape. This could give more information whether the chemical composition, the size or the shape of nanoparticles is the predominant factor in their tissue distribution.

5. Conclusion

We have demonstrated that the distribution of gold nanoparticles is size-dependent, the smallest particles showing the most widespread organ distribution including blood, heart, lungs, liver, spleen, kidney, thymus, brain, and reproductive organs. With the obtained results no reliable prediction about the distribution pattern can be made outside the tested size range. Therefore further kinetic and toxicokinetic studies are required to extend the existing knowledge on particle behavior in vivo.

Acknowledgements

We thank Dr. J. Sabine Becker, Research Centre Jülich, Jülich, Germany, for her support and the scientific discussions about ICP-MS. We also acknowledge the excellent technical assistance of Mrs. Trudy Riool – Nesselaar, Mrs. Liset De La Fonteyne and Mr. Henny Verharen.

References

[1] The Royal Society and The Royal Academy of Engineering. Nanoscience and nanotechnologies: opportunities and uncertainties. London, UK; 2004.
[2] Ballou B, Lagerholm BC, Ernst LA, Bruchez MP, Waggoner AS. Noninvasive imaging of quantum dots in mice. Bioconjug Chem 2004;15:79–86.
[3] Roszek B, De Jong WH, Geertsma RE. Nanotechnology in medical applications: state-of-the-art in materials and devices. RIVM report 265001001/2005. Bilthoven, The Netherlands; 2005.
[4] Singh R, Pantarotto D, Lacerda L, Pastorin G, Klumpp C, Prato M, et al. Tissue biodistribution and blood clearance rates of intravenously administered carbon nanotube radiotracers. Proc Natl Acad Sci U S A 2006;103:3357–62.
[5] Donaldson K, Stone V, Clouter A, Renwick L, MacNee W. Ultrafine particles. Occup Environ Med 2001;58:211–6.
[6] Oberdörster G, Oberdörster E, Oberdörster J. Nanotoxicology: an emerging discipline evolving from studies of ultrafine particles. Environ Health Perspect 2005;113:823–39.
[7] Hillyer JF, Albrecht RM. Gastrointestinal persorption and tissue distribution of differently sized colloidal gold nanoparticles. J Pharm Sci 2001;90:1927–36.
[8] Ji ZQ, Sun H, Wang H, Xie Q, Liu Y, Wang Z. Biodistribution and tumor uptake of $C_{60}(OH)_x$ in mice. J Nanopart Res 2006;8:53–63.
[9] Nemmar A, Hoet PH, Vanquickenborne B, Dinsdale D, Thomeer M, Hoylaerts MF, et al. Passage of inhaled particles into the blood circulation in humans. Circulation 2002;105:411–4.
[10] Oberdörster G, Sharp Z, Atudorei V, Elder A, Gelein R, Lunts A, et al. Extrapulmonary translocation of ultrafine carbon particles following whole-body inhalation exposure of rats. J Toxicol Environ Health A 2002;65:1531–43.

[11] Connor EE, Mwamuka J, Gole A, Murphy CJ, Wyatt MD. Gold nanoparticles are taken up by human cells but do not cause acute cytotoxicity. Small 2005;1:325–7.
[12] Kawano T, Yamagata M, Takahishi H, Niidome Y, Yamada S, Katayama Y, et al. Stabilizing of plasmid DNA in vivo by PEG-modified cationic gold nanoparticles and the gene expression assisted with electrical pulses. J Control Release 2006;111:382–9.
[13] Hainfeld JF, Slatkin DN, Smilowitz HM. The use of gold nanoparticles to enhance radiotherapy in mice. Phys Med Biol 2004;49:N309–15.
[14] Hirsch LR, Stafford RJ, Bankson JA, Sershen SR, Rivera B, Price RE, et al. Nanoshell-mediated near-infrared thermal therapy of tumors under magnetic resonance guidance. Proc Natl Acad Sci U S A 2003;100: 13549–54.
[15] Loo C, Lin A, Hirsch L, Lee MH, Barton J, Halas N, et al. Nanoshell-enabled photonics-based imaging and therapy of cancer. Technol Cancer Res Treat 2004;3:33–40.
[16] O'Neal DP, Hirsch LR, Halas NJ, Payne JD, West JL. Photo-thermal tumor ablation in mice using near infrared-absorbing nanoparticles. Cancer Lett 2004;209:171–6.
[17] Radt B, Smith TA, Caruso F. Optically addressable nanostructured capsules. Adv Mater 2004;16:2184–9.
[18] Hillyer JF, Albrecht RM. Correlative instrumental neutron activation analysis, light microscopy, transmission electron microscopy, and X-ray microanalysis for qualitative and quantitative detection of colloidal gold spheres in biological specimens. Microsc Microanal 1999;4:481–90.
[19] Niidome T, Yamagata M, Okamoto Y, Akiyama Y, Takahishi H, Kawano T, et al. PEG-modified gold nanorods with a stealth character for in vivo application. J Control Release 2006;114:343–7.
[20] Kreyling WG, Semmler M, Erbe F, Mayer P, Takanaka S, Schulz H. Translocation of ultrafine insoluble iridium particles from lung epithelium to extrapulmonary organs is size dependent but very low. J Toxicol Environ Health A 2002;65:1513–30.
[21] Kreyling WG, Semmler M, Moller W. Dosimetry and toxicology of ultrafine particles. J Aerosol Med 2004;17:140–52.
[22] Mills NL, Amin N, Robinson SD, Anand A, Davies J, Patel D, et al. Do inhaled carbon nanoparticles translocate directly into the circulatin in humans? Am J Respir Crit Care Med 2006;173:426–31.
[23] Wiebert P, Sanchez-Crespo A, Falk R, Philipson K, Lundin A, Larsson S, et al. No significant translocation of inhaled 35-nm carbon particles to the circulation in humans. Inhal Toxicol 2006;18:741–7.
[24] Cedervall T, Lynch I, Foy M, Berggård T, Donelly SC, Cagney G, et al. Detailed identification of plasma proteins adsorbed on copolymer nanoparticles. Angew Chem Int Ed 2007;46:5754–6.
[25] Geiser M, Rothen-Rutishauser B, Kapp N, Schürch S, Kreyling WG, Schulz H, et al. Ultrafine particles cross cellular membranes by nonphagocytic mechanisms in lungs and in cultured cells. Environ Health Perspect 2005;113:1555–60.
[26] Rothen-Rutishauser BM, Schürch S, Haenni B, Kapp N, Gehr P. Interaction of fine particles and nanoparticles with red blood cells visualized with advanced microscopic techniques. Environ Sci Technol 2006;40:4353–9.
[27] Geiser M, Rothen-Rutishauser B, Kapp N, Gehr P, Schürch S, Kreyling WG, et al. Ultrafine particles: Geiser et al. respond. Environ Health Perspect 2006;114:A212–3.
[28] Semmler M, Seitz J, Erbe F, Mayer P, Heyder J, Oberdorster G, et al. Long-term clearance kinetics of inhaled ultrafine insoluble iridium particles from the rat lung, including transient translocation into secondary organs. Inhal Toxicol 2004;16:453–9.